STÜSSI Heinrich — Dipl.-Ing.
SULZER BORTHERS LTD
Abt. 5 / Thermal Turbomachinery
Escher Wyss Platz
CH-8005 ZURICH (SWITZERLAND)

SUTER Peter — Professeur Dr.-Ing.
Institut de Thermique appliquée EPF-L
33 av. de Cour
CH-1007 LAUSANNE (SWITZERLAND)

SATOR Franz Georg — Dr.-Ing.
Institut d'Aérodynamique EPF-L
En Vernay
CH-1024 ECUBLENS (SWITZERLAND)

WOOD N. B. — Dr.-Ing.
Central Electricity Generating Board
Kelvin Avenue
LEATHERHEAD SURREY KT 22 7SE (ENGLAND)

Development and Application of a Conventional Combined Pressure, Temperature and Angle Probe with Small Dimensions

by

C. Güdel

1. INTRODUCTION

The development of modern axial compressor stages called for the provision of suitable probes, enabling the flow field to be measured - in particular between the individual blade rows too. Although the inherent problems of pneumatically indicating probes for measurements in rotary machines were known (i.e. unsteady impingement), this conventional metrology was retained. Another technique would in fact have been very welcome for measuring unsteady flow phenomena, but hot wire probes have too short a life under the flow velocities encountered, while the laser technique was not yet ripe for application at the time of this development project.

2. REQUIREMENTS

To accomodate all aspects (metrology, space conditions, reliability), probes meeting the following demands were needed:

- Small dimensions, to enable them to be traversed in an axial gap of 12 mm between rotor and stator blades maintaining a minimum safety clearance of about 3 mm. Fig. 1 shows the situation with an existing probe at the time and the new type to be developed.
- Simultaneous detection of:
  - total pressure and statistic pressure,
  - total temperature,
  - flow angle.

  This was necessary in view of the large number of detail measuring points and the high operating costs of the test machine.

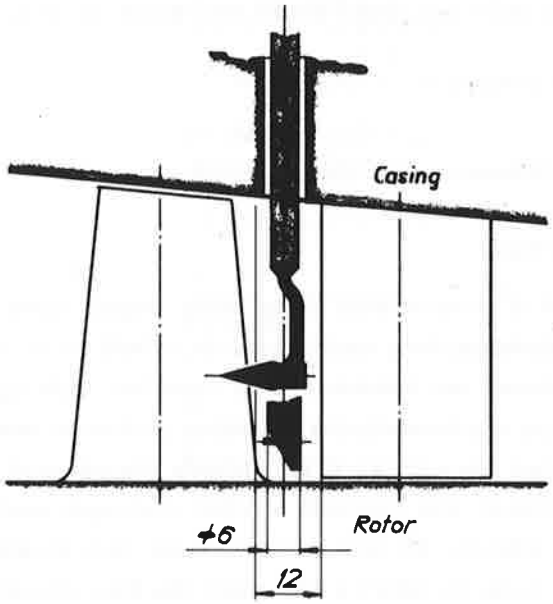

Fig. 1 Axial space configuration of the test compressor blading

3. DEVELOPMENT STEPS AND FINAL DESIGN

Figs. 2a - 2d show how the shape of the probe head was altered during the course of development. The reasons for the particular steps may be explained briefly as follows:

Variant 1 (Fig. 2a): - Very irregular calibration curves for the static pressure, so that clean interpolation was not possible.

- For the calibration curves of the pitch angle: no clear correlation between measured value and flow angle.
- Reading too sluggish.

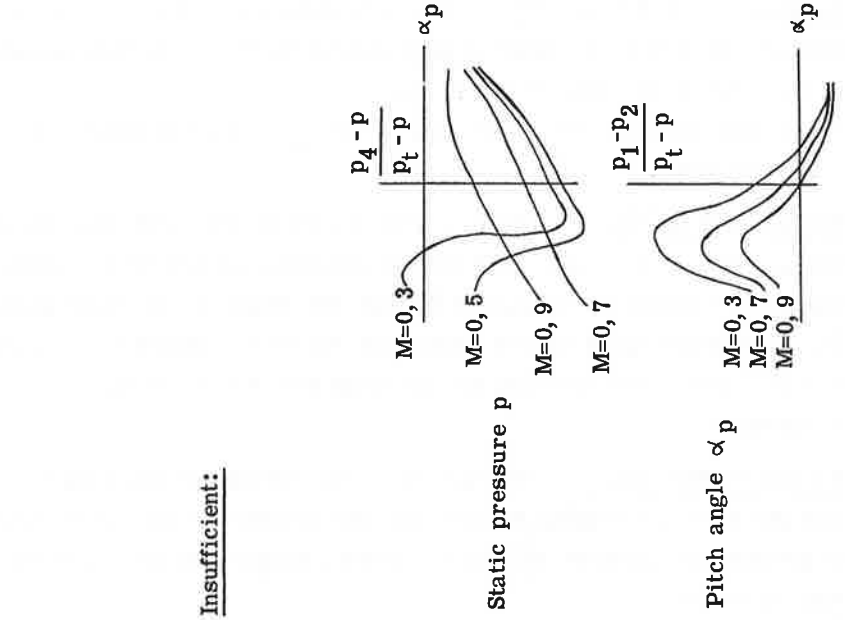

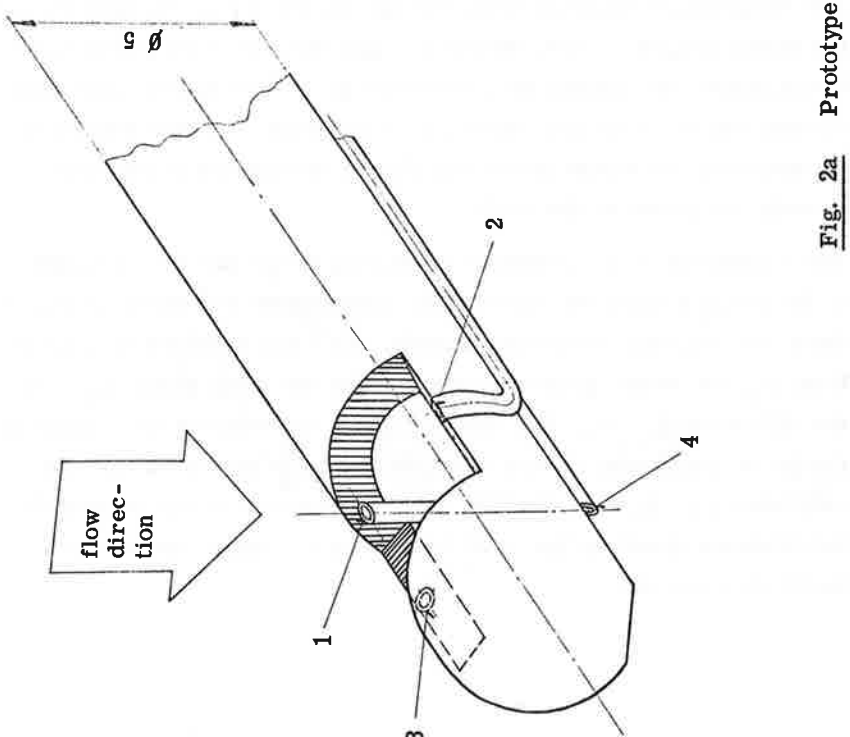

Fig. 2a Prototype 1

Variants 2 and 3 (Fig. 2b): - The only difference between these is that variant 3 has the wedge-shaped recess on the probe head bounded at an angle of 45^{o} instead of vertical.

- For both variants the calibration curves for the pitch angle are still unusable.

Variant 4 (Fig. 2c): - There is still a turn in the calibration curves for α_p at $\alpha_p \simeq -10^{o}$. This turn is probably caused by the probe shank, and cannot be influenced through the shape of the probe head. The application range of this probe was therefore limited to $\alpha_p = -10^{o}$ to $+10^{o}$, which was adequate for the proposed duty in an axial compressor.

Variant 5 (Fig. 2d): - The opening to the resistance thermometer was led from the sloping surface into the cylindrical part of the head, to prevent any possible influencing of the pressure measuring holes Nos. 2 and 3.

- This variant is largely identical with the final design (Figs. 3 and 4).

For temperature measurement, the air enters the probe head through the funnel-shaped orifice, streams round the four-wire resistance thermometer surrounded by a radiation protection sleeve, and exits through two slots in this sleeve, flowing round it on the outside as an additional insulation jacket and finally leaving the probe head through two ports on the back.

The numbering of the pressure measuring holes and the variables to be obtained from the appropriate measurands are shown in Fig. 5. Using the relevant calibration curves, the total pressure is obtained from p_1, the static pressure from p_4 and the pitch angle α_p from the difference $p_1 - p_2$. The yaw-angle α_y is indicated on a scale of the probe positioning device when the probe is turned so that the difference $p_2 - p_3 = 0$. Finally, the resistance R of the resistance thermometer gives us the total temperature - taking the recovery factor into account.

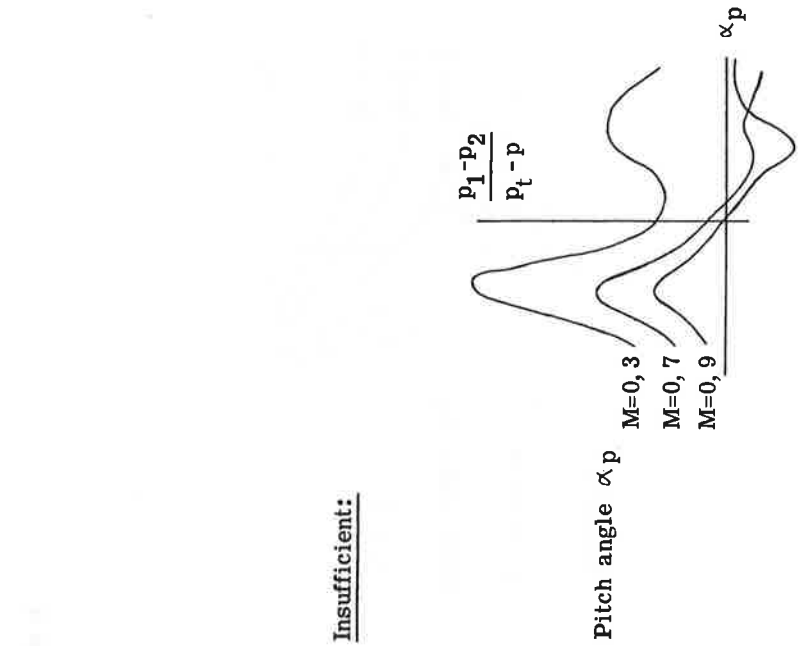

Fig. 2b Prototype 2/3

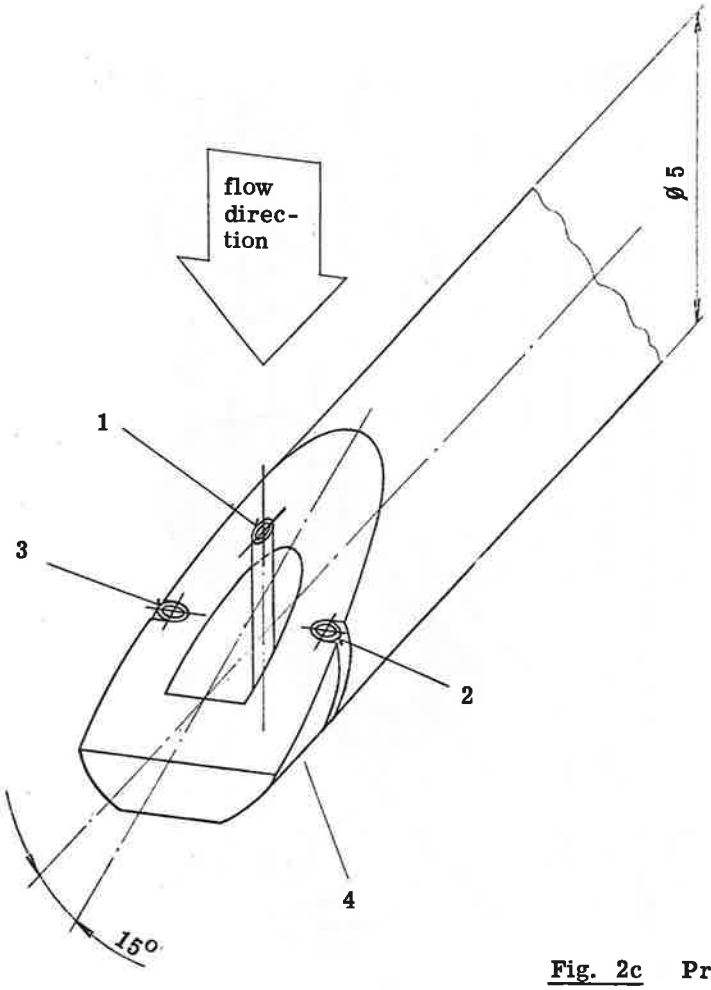

Fig. 2c Prototype 4

Sufficient:

Pitch angle α_p

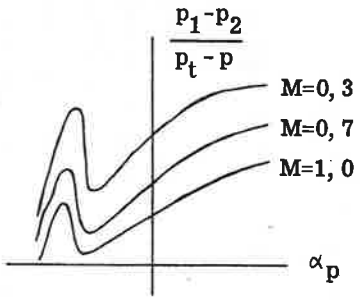

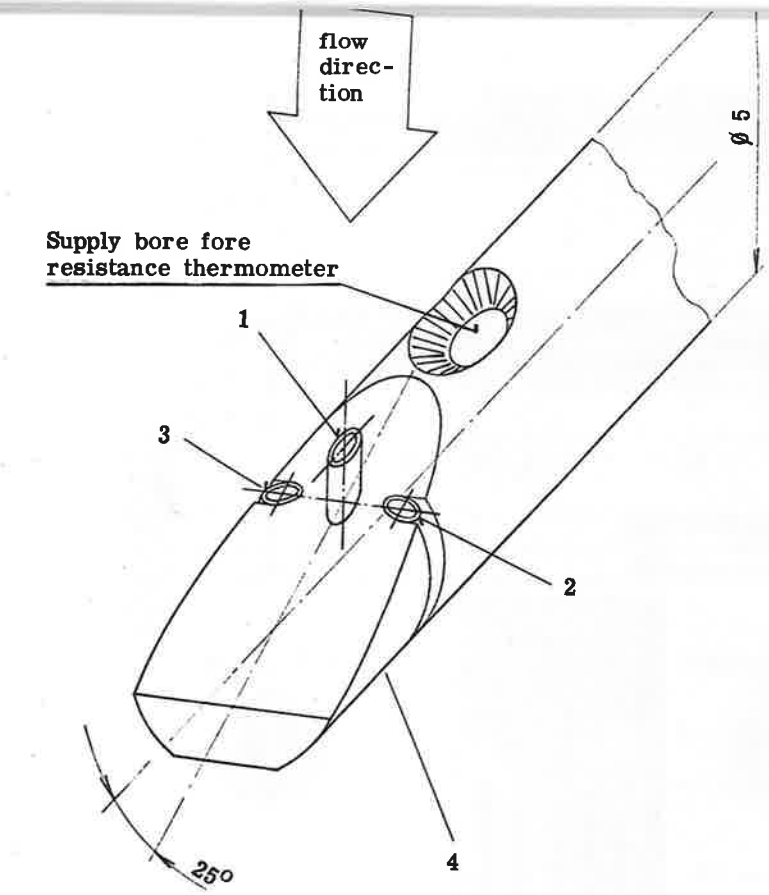

Fig. 2d Prototype 5

Improved:

Pitch angle α_p

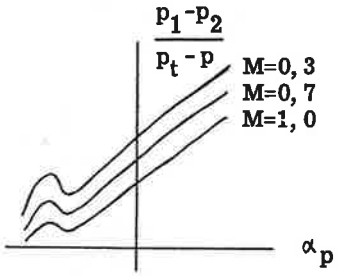

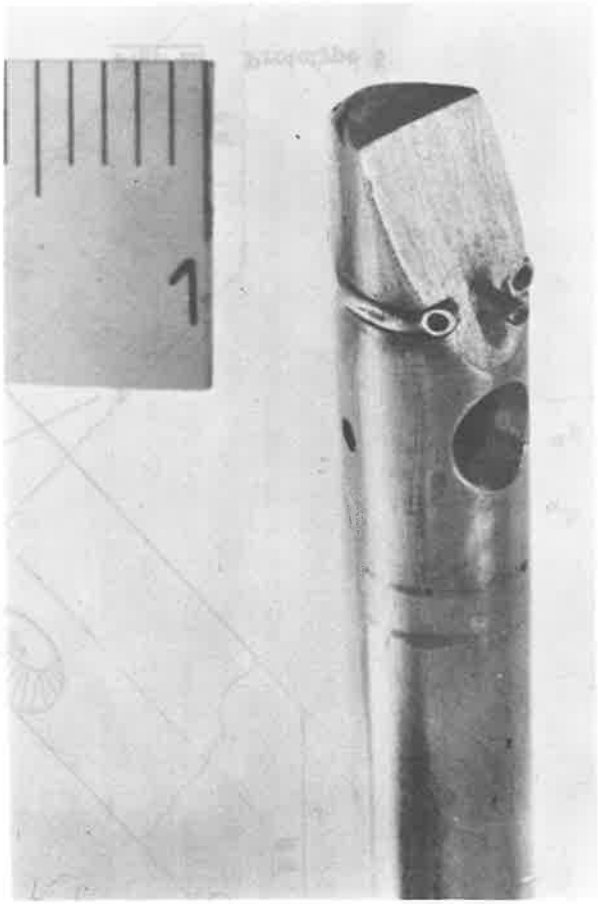

Fig. 3

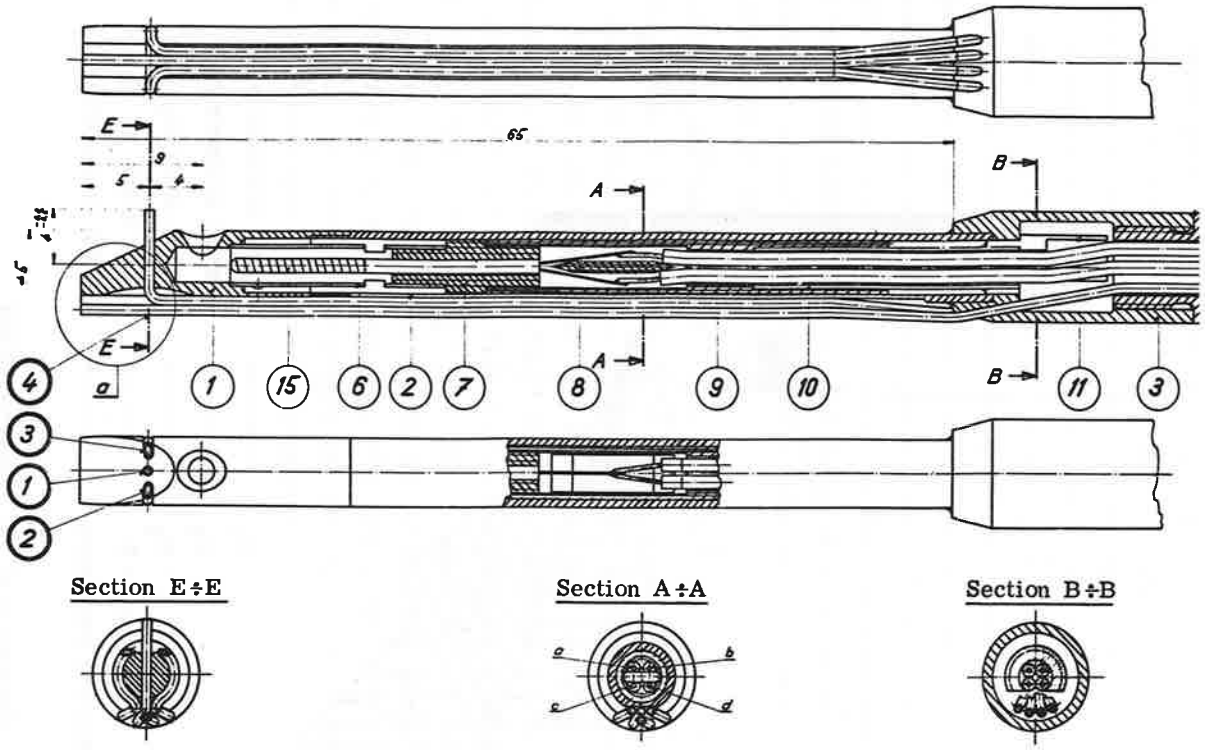

Fig. 4 Probe head

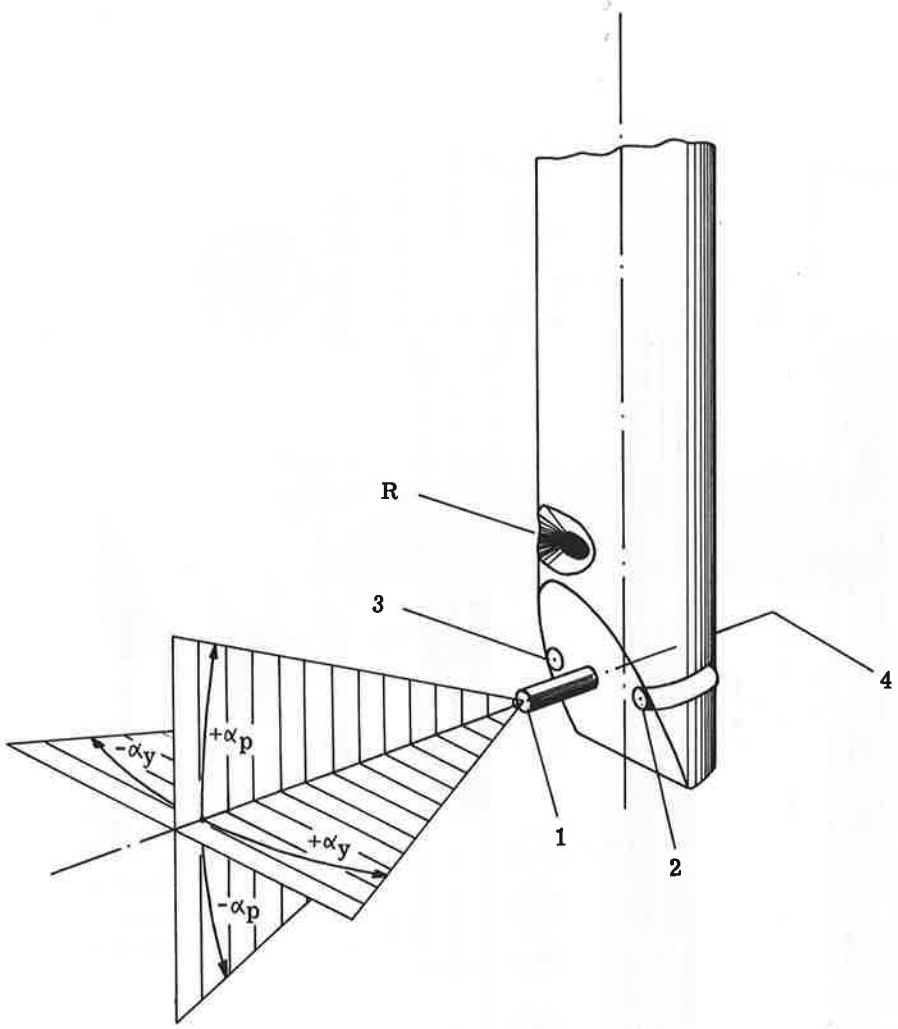

p_1 ⟶ Total pressure p_t

p_4 ⟶ Static pressure p

$p_1 - p_2$ ⟶ Pitch angle αp

$p_2 - p_3 = 0$ ⟶ Yaw angle αy

Electric resistance R ⟶ Total temperature T_t

Fig. 5 Evaluation of the measured values

4. CALIBRATION AND FURTHER INVESTIGATIONS

The new probe was calibrated on the probe calibration rig in the laboratory (Figs. 6 and 7). It produces a free jet streaming vertically downward with a diameter of 90 mm at the nozzle. Total pressure and temperature in the jet are assumed to be the same as in the chamber before the nozzle, where the flow velocity is very low. The static pressure is taken as equal to the ambient pressure, which had been confirmed by preliminary tests. By appropriate pressure increase in the chamber, jet velocities up to Mach 1 can be attained. The jet temperature can be varied from 30 to 120°C. The probe positioning device is remote-controlled on account of the high noise generation at high Mach numbers, and enables the probe to be turned about all three axes in space. For visual supervision of the probe in situ a TV camera may be installed.

The probe was calibrated for Mach numbers from 0.3 to 1.0 and for pitch angles from -10 to +10°. The results were evaluated with a computer program and plotted in a family of dimensionless curves, in which only the measurands p_1 to p_4 appear apart from the variable sought. As an example, in Fig. 8 the probe calibration curves for static pressure are shown. Plotted along the abscissa is the expression $\frac{p1 - p2}{p1 - p4}$, on the ordinate $\frac{p - p4}{p1 - p4}$, with the expression $\frac{p4}{p1}$ selected as parameter. This presentation enables the probe measurement to be evaluated at once, without iteration. The data of the probe calibration curves and the evaluation procedure are available as a subroutine and can be implemented in any computer program.

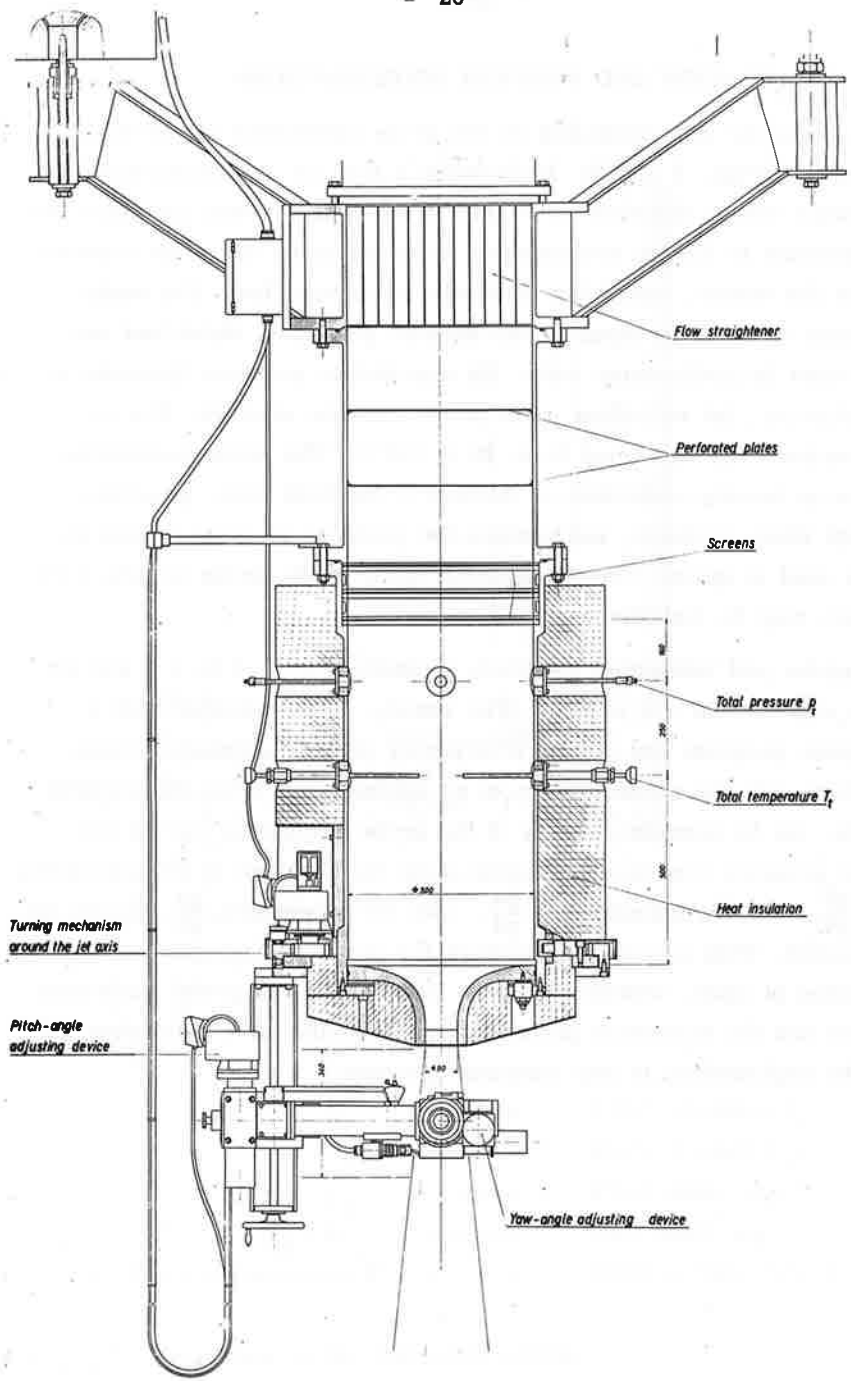

Fig. 6 Probe calibration rig

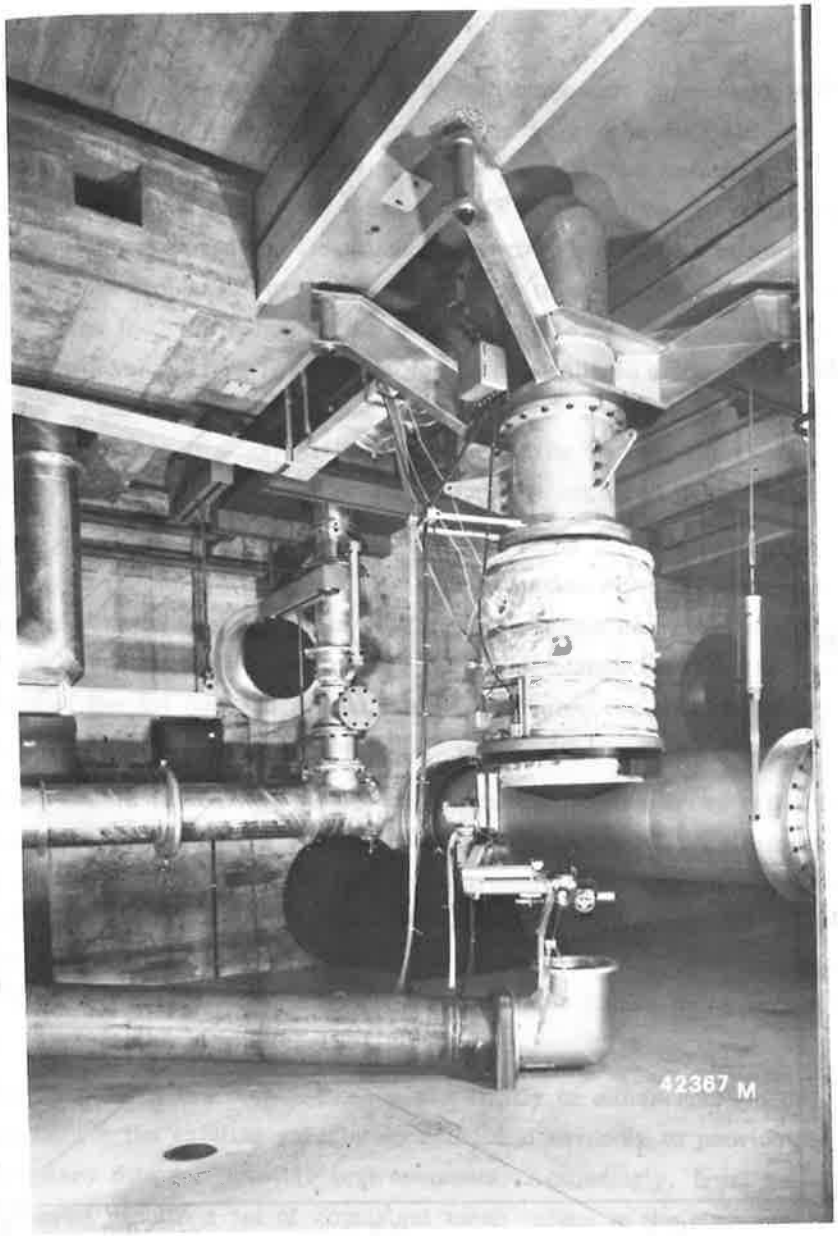

Fig. 7

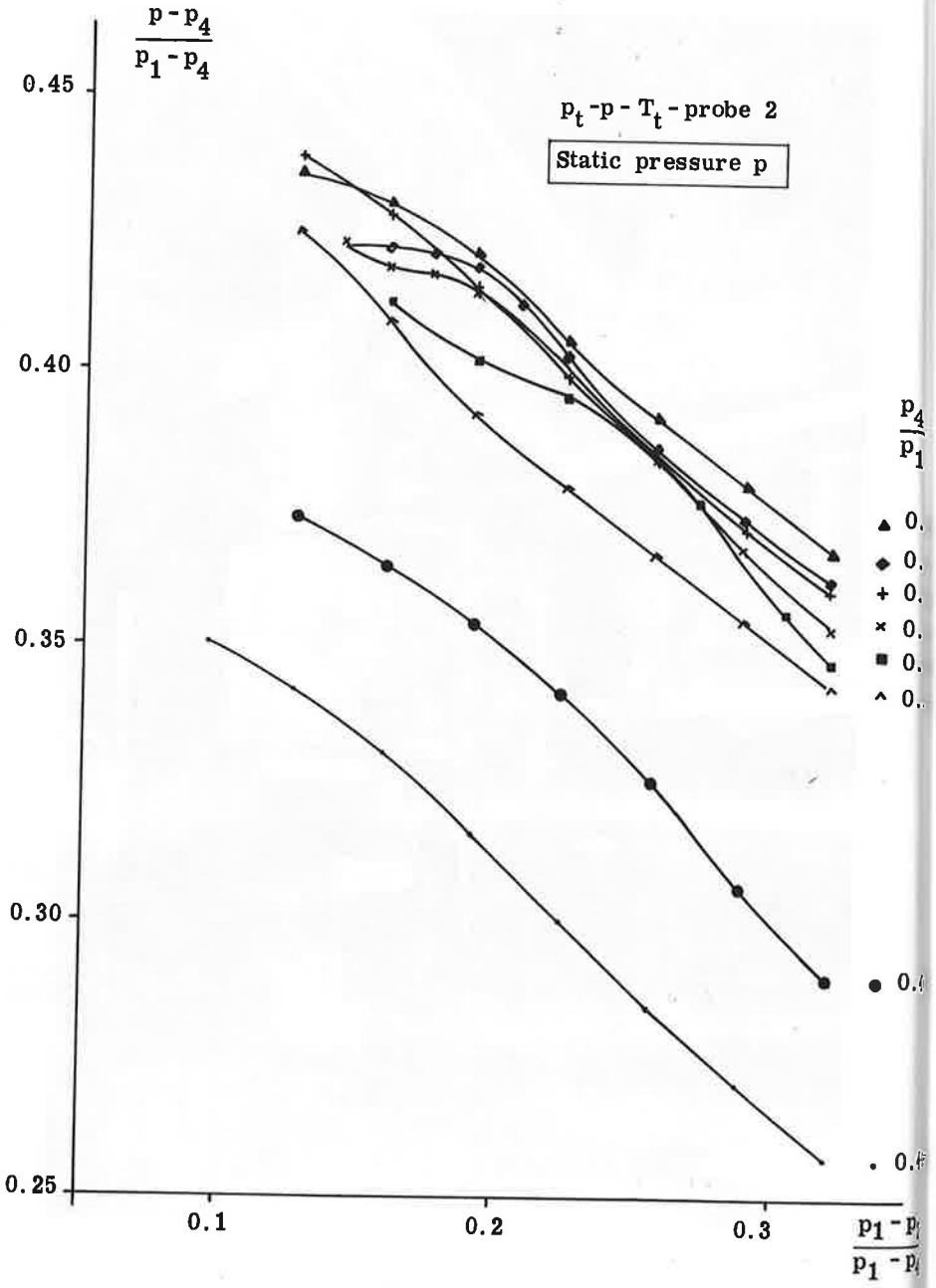

Fig. 8 Probe calibration chart

5. TYPICAL APPLICATION

Fig. 9 shows the blade passage of a multistage test compressor for air, in which the flow was measured with the new probe. Although the absolute flow velocity throughout the passage was well below Mach 1 and thus within the working range of the probe, together with the peripheral speed the flow onto the first row of blades becomes transsonic. To enable probe measurements to be performed after the last stage too, the height of the passage had to be made suitably large. The large volume flow resulting from this necessitated a power input up to 6 MW. This high energy consumption made the measuring operation very costly, so that any artifice to shorten the running time - by simultaneous probe indications for example - appeared desirable.

A nozzle for measuring the flow rate is located in the supply pipe upstream of the compressor. For overall measurements pressure and temperature measuring points are arranged in the entry and exit ducts. Probe measurements were carried out in all planes between the blade rows of the 1st and 2nd stages, as well as after the last row of stator blades. As operating point the design point was run in all cases.

Exact registration of the flow state within the blading array called for peripheral traverses on various radii as a fundamental requirement. In this way the variation of the static pressure over the pitch and the wakes behind the stator blades could be detected properly. The peripheral traverses were effected by the probe remaining on a radius in a fixed mounting and the adjacent row of stator blades being turned by one pitch in the circumferential direction.

The purpose of the measurements was firstly to either confirm or supplement the existing calculation data, and secondly to provide the necessary data for possible improvements. Accordingly, from the measured results a set of consistent mean values in the circumferential direction was defined for a fictitious equivalent flow of rotational symmetry. As a typical example, Fig. 10 shows the results in plane 11

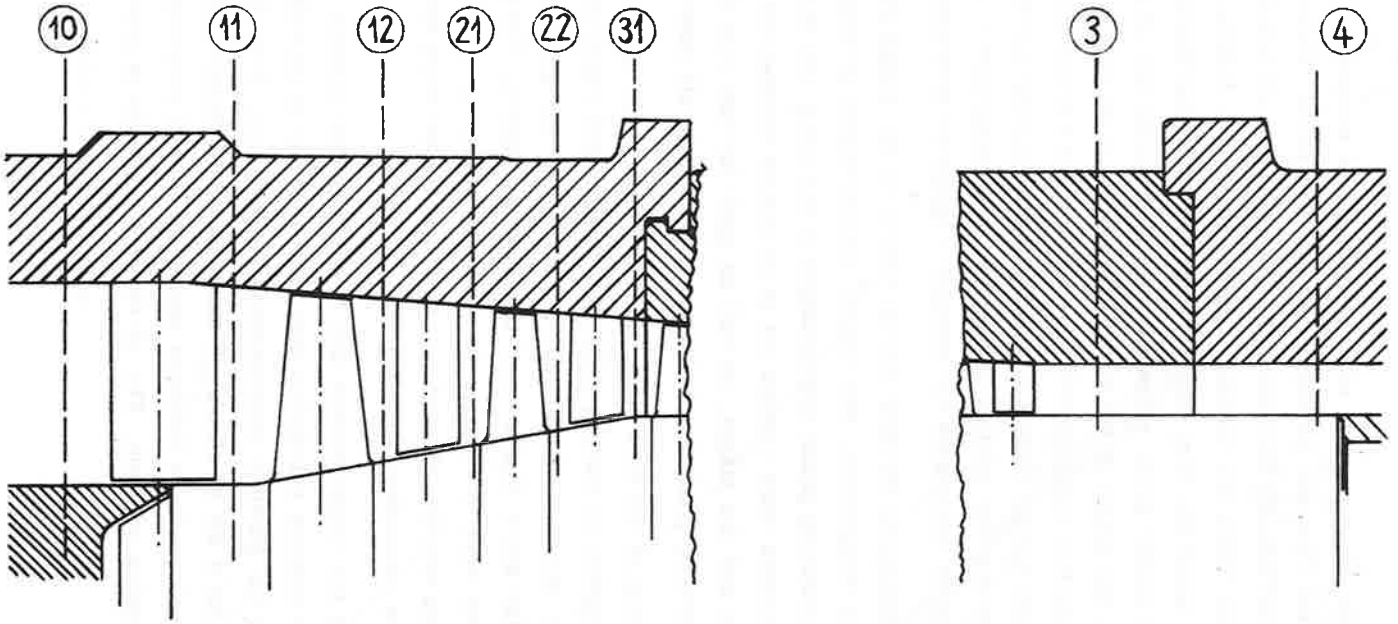

Fig. 9 Blade-channel of the test compressor

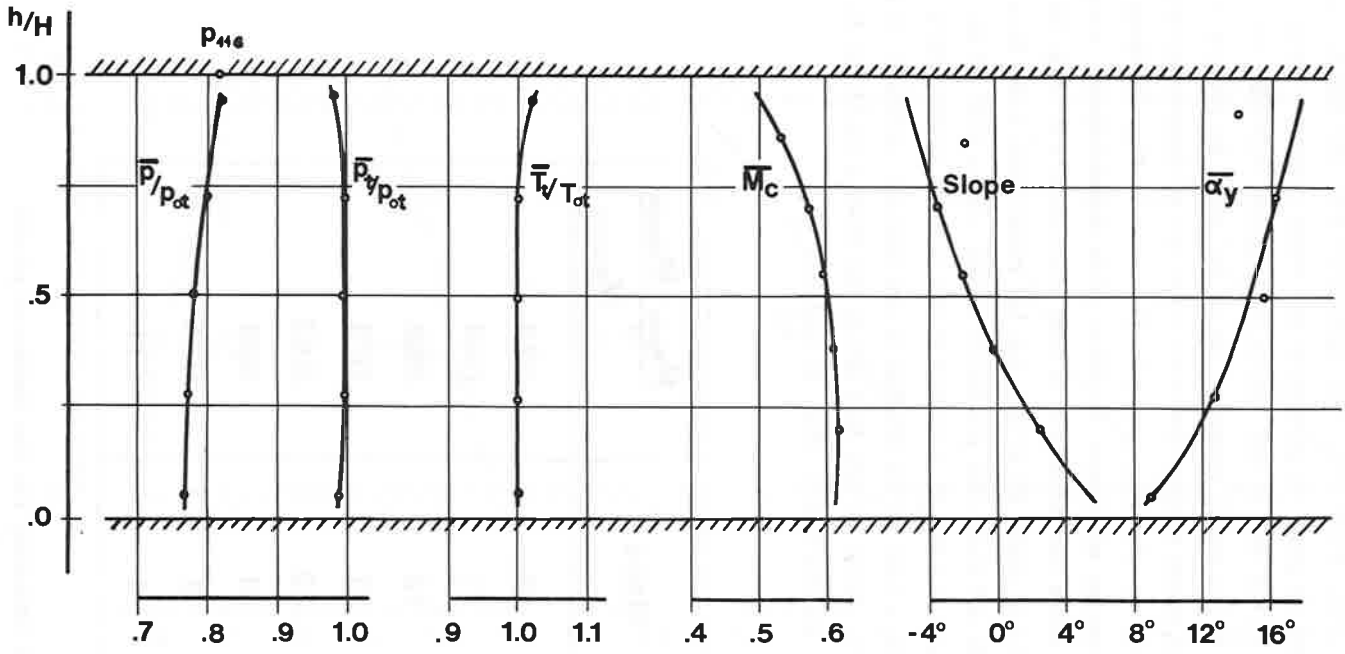

Fig. 10 Results of probe measurements in plane 11

before the first rotor blade row. The agreement with the design data may be described as good. In particular the static pressure curve extrapolated up to the wall of the casing also agrees well with the value indicated by the static pressure tap of the wall. By integration over the passage cross section the mass flow can be determined and compared with the nozzle measurement. The table in Fig. 11 shows the mass balances for all planes in which probe measurements were made. In most cases the difference is less than about 4%. Fig. 12 shows the results in plane 12 after the 1st rotor blade row. Here the pressures do not reach the predicted values. and a shift of the mass flow towards the hub is apparent in the velocity profile (Mc). Obviously the outer part of the blading is not working optimally. It is suspected that the cause of this lies not in the blading itself but in the periodically varying inflow (Fig. 13 and 14).

Plane	$\frac{\dot{M}_{Probe} - \dot{M}_{Nozzle}}{\dot{M}_{Nozzle}}$
10	.023
11	.044
12	.058
21	.073
22	.043
31	.039
3	-.026
4	-.011

Fig. 11 Mass balancing for the measured planes

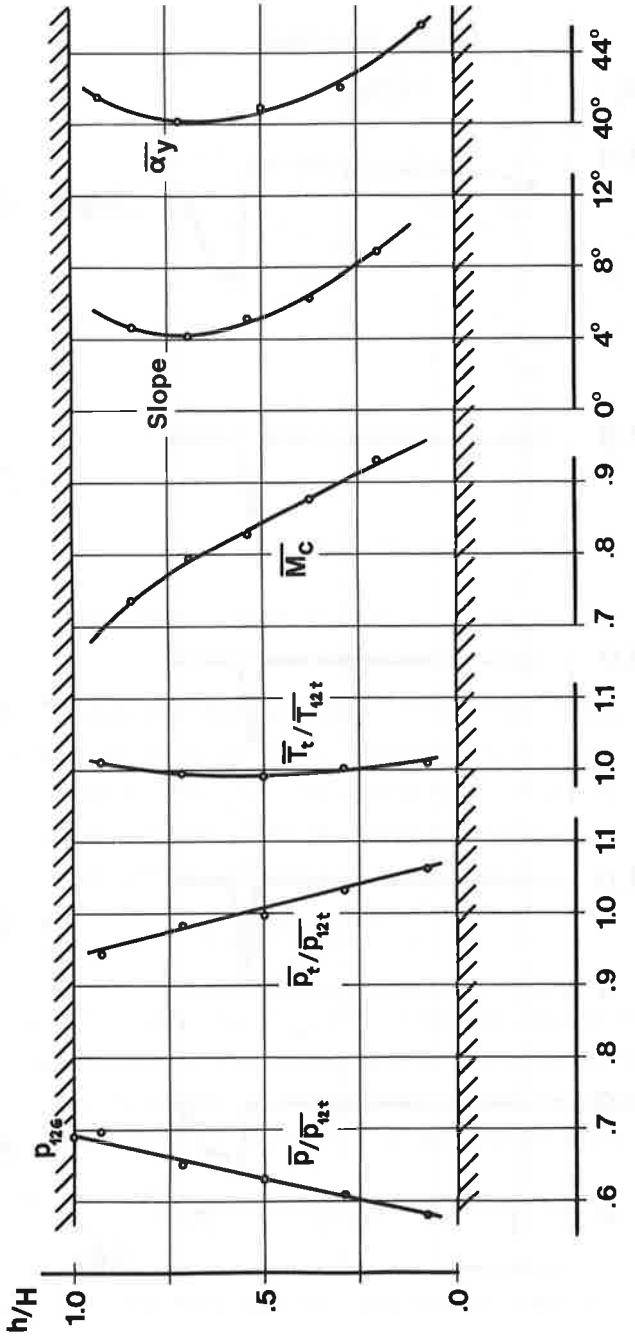

Fig. 12 Results of probe measurements in plane 12

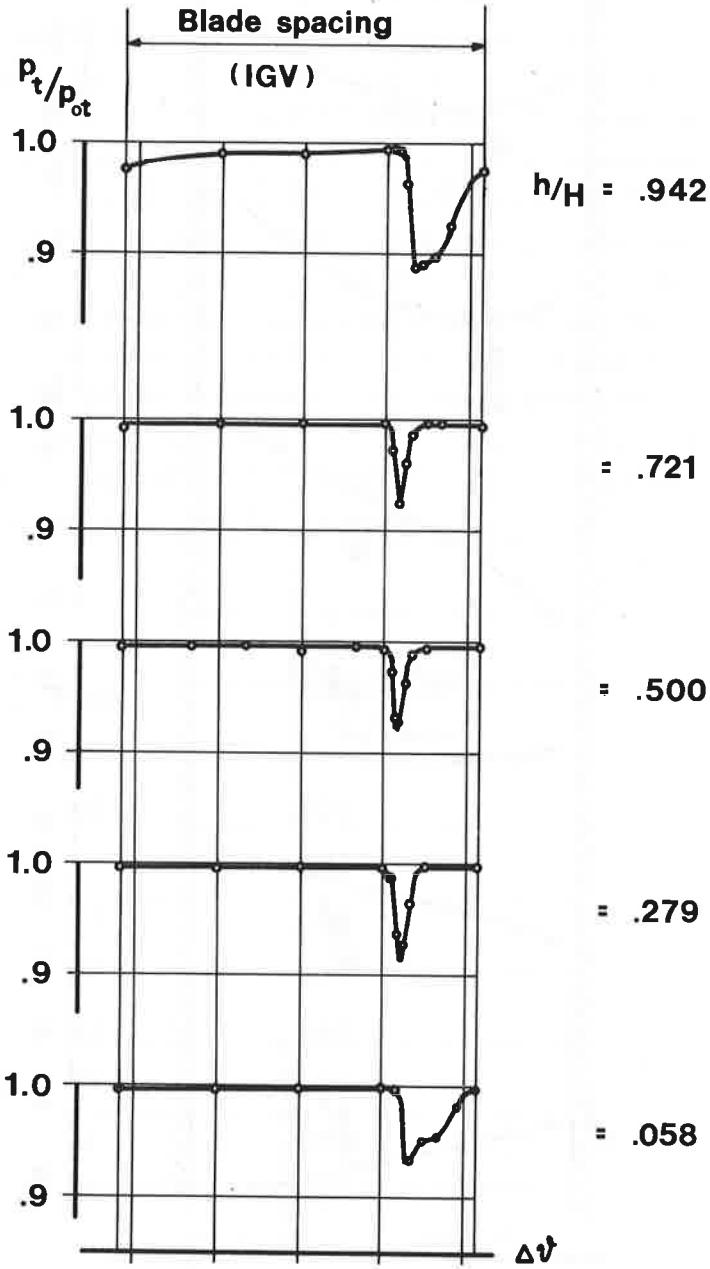

Fig. 13 Total pressure distribution behind inlet guide vane

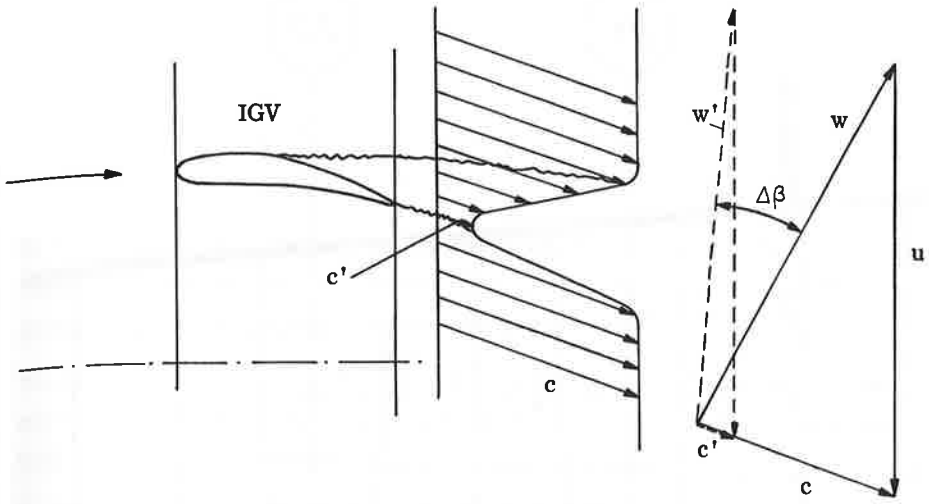

Fig. 14 Velocity diagram in front of 1st stage rotor blades (plane 11)

Further evidence of the reliability of the probe measurements is a comparison of the power input, made in this case on the rotor blading of the 2nd stage (Fig. 15). The direct temperature rise ΔT_t of the fluid measured by the probe is compared with a temperature increase calculated by means of Euler's turbine equation:

$$\Delta T_{Euler} = \frac{U_{22} \cdot Cu_{22} - U_{21} \cdot Cu_{21}}{Cp} \qquad (1)$$

The velocity components Cu_{21}, Cu_{22} in (1) are also derived from the probe measurement. The comparison is therefore between direct temperature measurement (with the resistance thermometer) and angle measurement. With one exception, the differences are of the order of:

$$\frac{\Delta T_t - \Delta T_{Euler}}{\Delta T_t} = \pm 0.02$$

In each case the entry and exit data are allocated to the same streamlines derived from the test.

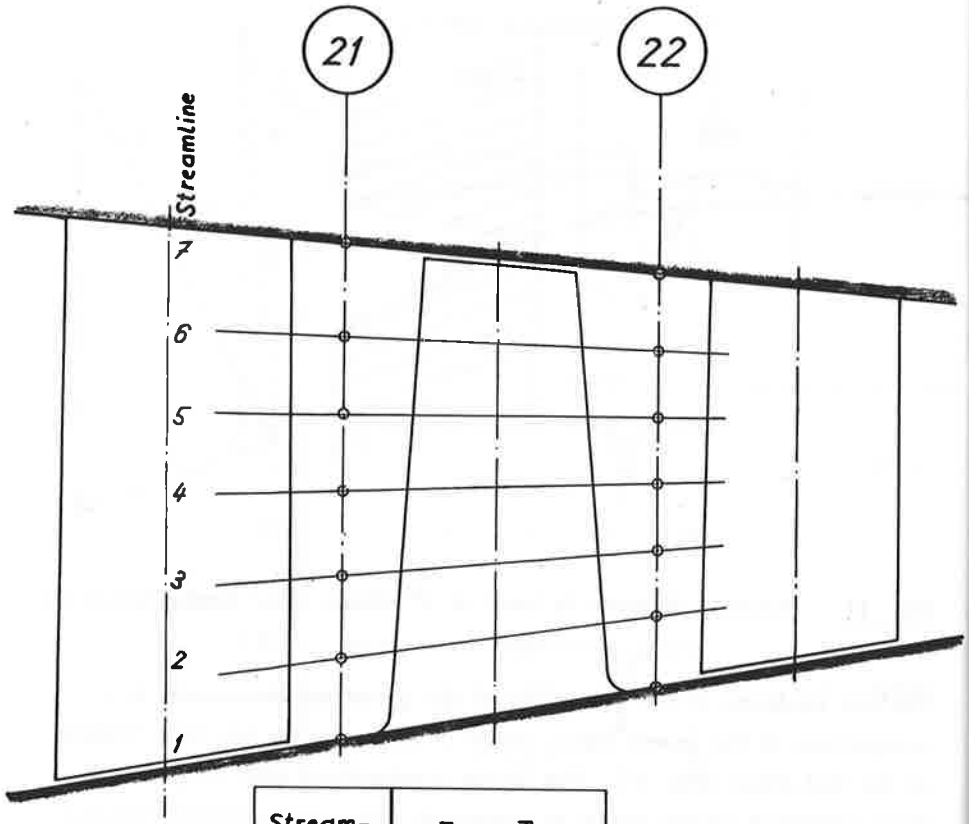

Stream-line	$\frac{\Delta T_t - \Delta T_{EULER}}{\Delta T_t}$
2	− 0.0234
3	− 0.0129
4	+ 0.0172
5	+ 0.0489
6	− 0.0029

ΔT_t = measured value

$\Delta T_{EULER} = \frac{u_{22} c_{u22} - u_{21} c_{u21}}{c_p}$

Fig. 15 Measured total temperature rise compared with temperature rise calculated from velocity diagrams (2^{nd} stage rotor)

Multi-parameter approximation of calibrating values for multi-hole probes

by

H. E. Gallus and D. Bohn

In this contribution there is presented a method for calculating the calibration spheres and calibration spaces of subsonic and supersonic probes by multiparameter approximation functions.

To determine the flow vector in both magnitude and direction, probes are normally used, which have special features, due to the measuring task.

In Fig. 1 there are shown the two types of five-hole-probes used for our measurements: On the left hand a semi-spherical five-hole-probe, normally adapted for subsonic measurements, and on the right hand, a conical five-hole-probe, used for supersonic flow measurements. Beneath the probe head, there are located two NTC-thermistors for measuring the flow temperature.

The probes presented here deliver seven informations independent from each other. Thus, seven flow parameters can be uniquely determined, as follows:

total pressure p_t
static pressure p
flow velocity c (Mach-number M)
the two angles of flow vector α, β
total temperature T_t
static temperature T